Naringin ameliorates intestinal injury in ulcerative colitis model mice by modulating the JAK2/STAT3 signaling pathway

MIAOMIAO WU[1,2*], YATING AN[3*], YONGMIN LI[4], WEI HE[5], YING WANG[5], YAQI WANG[3] and CAIXIA WU[5]

[1]College of Pharmacy, Hebei North University, Zhangjiakou, Hebei 075000, P.R. China;
[2]Hebei Key Laboratory of Neuropharmacology, Hebei North University, Zhangjiakou, Hebei 075000, P.R. China;
[3]Pharmaceutical Department, Tianjin Academy of Traditional Chinese Medicine Affiliated Hospital, Tianjin 300120, P.R. China;
[4]College of Traditional Chinese Medicine, Hebei University of Chinese Medicine, Shijiazhuang, Hebei 050200, P.R. China;
[5]College of Traditional Chinese Medicine, Hebei North University, Zhangjiakou, Hebei 075000, P.R. China

Received July 1, 2025; Accepted December 2, 2025

DOI: 10.3892/mmr.2026.13805

Abstract. Ulcerative colitis (UC) is a chronic autoimmune disease characterized by mucosal inflammation and disruption of the intestinal barrier. Current therapies often produce adverse effects, underscoring the need for novel treatment options. Naringin, a flavonoid from *Citrus aurantium* L., has shown anti-inflammatory potential in inflammatory bowel disease. However, its role in UC via the Janus kinase 2 (JAK2)/signal transducer and activator of transcription 3 (STAT3) pathway remains elusive. The present study investigated the therapeutic effects of naringin on UC, with a focus on JAK2/STAT3 signaling and intestinal barrier restoration. The present study employed a dextran sulfate sodium (DSS)-induced colitis mouse model and IL-6-stimulated Caco-2 cells. Mice were administered 3% DSS for 10 days along with naringin (40 mg/kg) or mesalazine (0.2 g/kg) treatment. Disease activity index (DAI), histopathology, expression of tight junction proteins zona occludens-1 (ZO-1) and occludin and JAK2/STAT3 pathway protein activation were evaluated. In Caco-2 cells, transepithelial electrical resistance (TEER) and fluorescein isothiocyanate-dextran 4 kDa (FD-4) permeability assays assessed barrier function, with STAT3 silencing supporting pathway involvement. Naringin markedly alleviated DSS-induced colitis, reducing weight loss, colon shortening, DAI and histological scores. Furthermore, naringin restored ZO-1 and occludin expression while suppressing JAK2/STAT3 phosphorylation in colon tissues. In Caco-2 cells, naringin reversed IL-6-induced reductions in TEER and increases in FD-4 permeability, while enhancing tight junction fluorescence. Furthermore, STAT3 silencing in combination with naringin led to a further decrease in the p-JAK2/JAK2 ratio compared with that in the IL-6 group (though to a lesser extent than naringin alone), consistent with the involvement of the JAK2/STAT3 pathway. Collectively, these findings demonstrate that naringin ameliorates UC by promoting intestinal barrier repair through suppression of JAK2/STAT3 activation, highlighting its therapeutic potential for UC.

Introduction

Ulcerative colitis (UC) is a chronic inflammatory bowel disease (IBD) primarily affecting the colon which is characterized by mucosal inflammation. Its incidence is gradually increasing worldwide, with rates in China reaching 11.6 per 100,000 individuals (1,2). If left untreated UC can progress to colorectal cancer or result in systemic complications (3). The pathogenesis of UC involves immune dysregulation, excessive production of pro-inflammatory cytokines and gut microbiota imbalance (4). Current first-line therapies include aminosalicylates, such as mesalazine, corticosteroids and immunomodulators. However, up to 50% of patients experience treatment-related adverse events, such as glucose intolerance and hepatotoxicity (5), highlighting the need for safer and more effective therapeutic alternatives. Natural products have therefore attracted growing attention as potential candidates (6,7).

The intestinal barrier serves an important role in the pathogenesis of UC. Disruption of its structural and functional integrity contributes to increased intestinal permeability, microbial translocation and sustained immune activation. Growing evidence suggests that enhancing intestinal barrier

Correspondence to: Professor Wei He, College of Traditional Chinese Medicine, Hebei North University, 11 South Diamond Road, Hi-Tech Industrial Development Zone, Zhangjiakou, Hebei 075000, P.R. China
E-mail: 18032319958@163.com

Miss Yaqi Wang, Pharmaceutical Department, Tianjin Academy of Traditional Chinese Medicine Affiliated Hospital, 354 North Road, Hongqiao, Tianjin 300120, P.R. China
E-mail: tjwangyaqi@sina.com.cn

*Contributed equally

Abbreviations: JAK2, Janus kinase 2; STAT3, signal transducer and activator of transcription 3; UC, ulcerative colitis

Key words: naringin, ulcerative colitis, JAK2/STAT3 signaling pathway, intestinal mucosal barrier, *Citrus aurantium* L.

function represents a promising therapeutic strategy for UC (8-14). Among the signaling mechanisms implicated, the Janus kinase 2 (JAK2)/signal transducer and activator of transcription 3 (STAT3) pathway has been extensively studied. Hyperactivation of this pathway is a hallmark of UC, contributing to both inflammation and barrier dysfunction (15,16). The preliminary data of the present study (data not shown), together with prior reports (17,18), have suggested that naringin, a natural flavonoid, may exert anti-inflammatory effects through modulation of kinase signaling pathways. The present study therefore focused on the JAK2/STAT3 pathway to elucidate the mechanism underlying its protective activity.

Citrus aurantium L., a member of the Rutaceae family also known as bitter orange, is widely consumed in China as both a food and traditional medicine, owing to its anti-inflammatory properties (18). Previous studies have demonstrated that *Citrus aurantium* L. alleviates trintrobenzene sulfonic acid (TNBS)-induced IBD in rats, while its major flavonoid naringin reduces the expression of inducible nitric oxide synthase (iNOS), cytochrome c oxidase subunit 2 (COX-2) and TNF-α (17,18). Naringin has also been shown to ameliorate clinical symptoms in murine models of IBD (17,18). Given that the JAK2/STAT3 pathway is hyperactivated in UC and promotes inflammation (15,16), its pharmacological inhibition has emerged as a promising therapeutic approach (19-21). However, the role of naringin in modulating UC through this pathway remains undefined. The present study aimed to investigate the effects of naringin on sodium sulfate dextran (DSS)-induced colitis and its influence on the JAK2/STAT3 signaling pathway.

Materials and methods

Materials. Naringin (cat. no. B21594-1g; Shanghai Yuanye Bio-Technology Co., Ltd.) and fluorescein isothiocyanate dextrose 4000 (FD-4; molecular weight, 3,000-5,000 kDa; cat. no. FD4-250MG) were purchased from Sigma Chemical Co. Mesalazine (cat. no. 20230605) was obtained from Heilongjiang Tianhong Pharmaceutical Co., Ltd. DSS (molecular weight, 36,000-50,000 kDa; cat. no. 02160110-CF) was purchased from MP Biomedicals, LLC. Caco-2 cells were obtained from Cell Resource Center, Peking Union Medical College. Cell culture reagents (HyClone™; Cytiva) included modified Eagle's medium (MEM; cat. no. SH30024.01), fetal bovine serum (FBS; cat. no. SH30071.03) and penicillin-streptomycin (cat. no. SV30010).

Animals. Healthy male BALB-c mice (aged 6-8 weeks; 18-22 g) were obtained from Sbeifu (Beijing) Biotechnology Co., Ltd. (certificate of conformity no. 110324210106095731). Mice were housed in cages with controlled temperature (22±2˚C), relative humidity (40-60%) and a 12-h light/dark cycle throughout the study. All mice were fed a standard diet (crude protein 16%, crude fat 4%, crude fiber 12% and ash 8%) and had free access to water. Animal experiments were approved by the Animal Welfare Committee of Hebei North University (Zhangjiakou, China; approval no. HBNV20240223003) and performed according to institutional guidelines.

DSS-induced colitis mice. A total of 32 mice were randomly divided into four groups, each consisting of eight mice: The normal, control, mesalazine control and naringin groups. Intragastric administration volumes were 0.3 ml per 10 g body weight. Mesalazine and naringin were suspended in 5% acacia gum (cat. no. V900768-500G; MilliporeSigma; Merck KgaA) and the final doses were 0.2 g/kg and 40 mg/kg, respectively. The dose of 40 mg/kg naringin was selected based on previous studies demonstrating efficacy in rodent models of colitis (17,18). Similarly, the mesalazine dose of 0.2 g/kg is a standard dose used in DSS murine models (22,23). Except for the normal group, all the other groups were freely administered 3% DSS (dissolved in drinking water) to establish the UC mouse model, which was administered alongside other treatments (22,23). The naringin and mesalazine groups received their respective drug suspensions (in 5% acacia gum) by oral gavage once daily for 10 days. The normal and control groups received an equivalent volume of the vehicle (5% acacia gum solution) on the same schedule. Diet and hydration, body movement, body weight, diarrhea incidence and bloody stool were recorded daily throughout the present study.

Disease activity index (DAI) and analysis of colon injury. Body weight, stool character and incidence of bloody stools were recorded daily after models were established. The DAI was determined using a previously established scoring system (Table I) (24). On day 11, mice were anesthetized via inhaled isoflurane (induction, 4%; maintenance, 1.5-2% in oxygen) delivered by a precision vaporizer for final blood collection from the retro-orbital plexus. A terminal blood sample not exceeding 10% of total blood volume (0.6-0.8 ml) was collected. Following this, pentobarbital sodium (40 mg/kg) was administered by intraperitoneal injection to ensure a surgical plane of anesthesia, confirmed by the loss of pedal reflex, before euthanasia was performed via cervical dislocation. This approach guaranteed the absence of pain or distress throughout the procedure. Death was verified by the cessation of cardiac and respiratory activity. All animal procedures were strictly performed in accordance with the approved animal protocol. The colon segment was resected to evaluate the macroscopic colon injury, which was scored according to the method reported in the literature (Table II) (18). Routine hematoxylin and eosin-stained colon sections, according to previously described morphological criteria and observed colon tissue damage, were assessed blindly by two investigators according to a modified histological grading scale, which considered both inflammatory cell infiltration and tissue damage (Table III) (18). Any discrepant scores were resolved through a joint re-evaluation of the slide under a multi-head microscope to reach a consensus. If a consensus could not be reached, a third experienced pathologist was consulted for a final decision.

Western blot analysis for JAK2/STAT3 signaling pathway-related proteins from colon tissues. To determine the protective effect of naringin, western blot analysis was performed. Colon tissues were homogenized in RIPA buffer (cat. no. P0013B; Beyotime Biotechnology) supplemented with 1% (v/v) Protease and Phosphatase Inhibitor Cocktail (cat. no. P1050; Beyotime Biotechnology). Protein concentrations were measured using Cytation 5 (BioTek; Agilent Technologies, Inc.) using a bicinchoninic acid (BCA) protein

Table I. Evaluation of DAI scores.

DAI score	Weight loss, %	Stool consistency	Occult or gross bleeding
0	None	None	None
1	1-5	Loose	Hemoccult positive
2	5-10	Loose	Hemoccult positive
3	10-15	Diarrhea	Gross bleeding
4	>15	Diarrhea	Gross bleeding

DAI, disease activity index.

Table II. Evaluation of macroscopic scores.

Colon damage	Score
No damage	0
Hyperemia with ulcers	1
Hyperemia and wall thickening without ulcers	2
One ulceration site without wall thickening	3
Two or more ulceration sites	4
0.5 cm extension of inflammation or major damage	5
1 cm extension of inflammation or severe damage	6-10

Table III. Evaluation of histological scores.

A, Inflammatory cell infiltration	
Pathological characteristic	Score
No infiltration	0
Increased number of inflammatory cells in the lamina propria	1
Inflammatory cells extending into the submucosa	2
Transmural inflammatory cell infiltration	3
B, Tissue damage	
Pathological characteristic	Score
No mucosal damage	0
Discrete epithelial lesions	1
Erosion or focal ulcerations	2
Severe mucosal damage with extensive ulceration extending into the bowel wall	3

assay kit (cat. no. PC0020; Beijing Solarbio Science & Technology Co., Ltd.). A total of 60 μg protein were mixed with 4X loading dye, as well as Laemmli buffer and 2-mercapto ethanol, and were heated at 95˚C for 5 min. The proteins were resolved by 8-12% SDS-PAGE and transferred to immunoblot PVDF membranes (cat. no. IPVH00010; Merck KGaA). The membranes were blocked with 5% non-fat dry milk in Tris-buffered saline containing 0.1% Tween-20 (TBST) for 2 h at room temperature, then incubated at 4˚C overnight with primary antibodies against IL-6 (1:1,000; cat. no. Bs-0782R; BIOSS), phosphorylated (p-)JAK2 (1:1,000; cat. no. bs-2485R; BIOSS), JAK2 (1:1,000; cat. no. bs-0908R; BIOSS), p-STAT3 (1:1,000; cat. no. bs-1658R; BIOSS), STAT3 (1:1,000; cat. no. bs-55208R; BIOSS), occludin (1:1,000; cat. no. A2601; ABclonal Biotech Co., Ltd.), zona occludens-1 (ZO-1; 1:1,000; cat. no. A0659; ABclonal Biotech Co., Ltd.) and β-actin (1:1,000; cat. no. ab8227; Abcam). The membranes were washed with TBST three times for 10 min each and incubated with a horseradish peroxidase (HRP)-labeled secondary goat anti-rabbit (1:5,000; cat. no. ab6721; Abcam) antibodies for 1 h at room temperature. After washing three times with TBST, bands were detected using ECL Plus Ultra-Sensitive Substrate (cat. no. PE0010; Beijing Solarbio Science & Technology Co., Ltd.) and visualized using the ChemiDoc MP Imaging System (Bio-Rad Laboratories, Inc.) after washing three times. The band intensities were semi-quantified using ImageJ v1.53 gel analysis software (National Institutes of Health).

IL-6-induced Caco-2 barrier injury model. Caco-2 cells were cultured in MEM supplemented with 20% FBS, penicillin (100 units/ml), streptomycin (100 μg/ml), L-glutamine (4.5 mg/ml) and glucose (4.5 mg/ml), and incubated at 37˚C in a humidified atmosphere containing 5% CO_2. The medium was refreshed every other day. A total of $2x10^6$ cells/ml Caco-2 cells were then seeded into a 24-well plate and incubated overnight at 37˚C. The following day, the medium was changed to a new medium containing 20 ng/ml IL-6 (cat. no. P05231; Boster Biological Technology) and cells were incubated for 45 min at 37˚C. This resulted in the formation of mucosal barrier damage in the Caco-2 cells.

Measurement of transepithelial electrical resistance (TEER) and FD-4 permeability. As described in previously published protocols (18) with slight modification, $1.5x10^5$ cells/ml Caco-2 cells were seeded in Transwell cell culture chambers (6.5 mm diameter inserts; 3.0 mm pore size; Costar; Corning, Inc.), and the growth medium was changed every 2 days. A monolayer of Caco-2 cells was formed after cells were cultured for 10 days. Subsequently, cells were incubated with or without IL-6 (20 ng/ml) for 45 min at 37˚C and incubated with naringin (40 μmol/l for 2 h at 37˚C. The cell culture was replaced with serum-free medium and incubated for another 30 min at 37˚C before the sample TEER (Ω/cm^2) was assessed.

After the detection of TEER, 100 ml of 1 mg/ml FD-4 was added into the Transwell upper chambers before the cells were incubated in 37˚C for 30 min. After that, 100 ml medium from the lower chamber of the Transwell was added into a black well to detect the fluorescence content at an excitation wavelength of 480 nm and emission wavelength of 520 nm using SpectraMax® M5 (Molecular Devices, LLC) as reported in a previous study (25).

Immunofluorescence assay. Cells were fixed with 4% paraformaldehyde (cat. no. BL539A; Beijing Lanjieke Technology Co., Ltd.) at room temperature for 30 min. After discarding the fixative, the cells were washed with Dulbecco's phosphate-buffered

saline and blocked with 5% bovine serum albumin sealing solution at room temperature for 2 h. For immunofluorescence experiments, cells were incubated with the primary antibodies ZO-1 (cat. no. A0659; ABclonal Biotech Co., Ltd.) and occludin (cat. no. A2601; ABclonal Biotech Co., Ltd.) at 1:200 dilution overnight at 4˚C after blocking. Cells were then washed with PBS containing 0.1% Tween-20 and subsequently incubated with goat anti-rabbit-Alexa Fluor 488 (1:500; cat. no. 4412S; CST Biological Reagents Co., Ltd.) and goat anti-rabbit-Alexa Fluor 647 (1:500; cat. no. 4414S, CST Biological Reagents Co., Ltd.) fluorescent secondary antibodies at room temperature for 2 h in the absence of light. Finally, cells were counter-stained with DAPI (cat. no. D1306; Thermo Fisher Scientific, Inc.) for 10 min, and the images were collected and analyzed using a laser confocal microscope (FV3000; Olympus Corporation).

Small interfering RNA (siRNA) transfection and western blot analysis in Caco-2 cells. siRNA targeting STAT3 (siSTAT3) and negative control siRNA (siNC) were purchased from Suzhou GenePharma Co., Ltd. The sequences were as follows: siSTAT3, sense 5'-CCCGGAAAUUUAACAUUCUTT-3', antisense 5'-AGAAUGUUAAAUUUCCGGGTT-3'; and siNC, sense 5'-UUCUCCGAACGUGUCACGUTT-3', antisense 5'-ACGUGACACGUUCGGAGAATT-3'. Caco-2 cells were transfected with siRNA using Lipofectamine® 3000 reagent (Invitrogen; Thermo Fisher Scientific, Inc.) according to the manufacturer's protocol. Briefly, Caco-2 cells were seeded at a density of $2x10^6$ cells/well in a 6-well plate. In each well, 100 pmol siRNA was complexed with Lipofectamine 3000 reagent. The transfection mixture was incubated with the cells for 6 h at 37˚C, after which it was replaced with fresh complete medium. A total of 24 h after transfection, the transfected cells were treated with IL-6 (20 ng/ml) for 45 min at 37˚C, followed by naringin (40 μmol/l) treatment for 2 h at 37˚C, prior to protein extraction. For protein detection, Caco-2 cells were lysed using ice-cold RIPA buffer (Thermo Fisher Scientific, Inc.) and centrifuged 12,000 x g for 5 min at 4˚C. Protein concentrations were determined using a BCA assay (Beyotime Biotechnology). Total proteins (20 mg/lane) were subjected to electrophoresis in a 12% polyacrylamide gel and transferred onto a PVDF membrane. Subsequently, the membrane was blocked at 37˚C for 1 h with 5% non-fat milk in TBS, with 0.05% Tween-20. Membranes were subsequently incubated separately with primary antibodies for p-JAK2 (1:1,000; cat. no. bs-2485R; BIOSS), JAK2 (1:1,000; cat. no. bs-0908R; BIOSS), p-STAT3 (1:1,000; cat. no. bs-1658R; BIOSS), STAT3 (1:1,000; cat. no. bs-55208R; BIOSS), occludin (1:1,000; cat. no. A2601; ABclonal Biotech Co., Ltd.), ZO-1 (1:1,000; cat. no. A0659; ABclonal Biotech Co., Ltd.) and β-actin (1:1,000; cat. no. ab8227; Abcam), and then with HRP-conjugated goat anti-rabbit IgG secondary antibody (1:5,000; cat. no. ab6721; Abcam). Signals were detected by enhanced chemiluminescence (Thermo Fisher Scientific, Inc.). Western blot images were semi-quantified using ImageJ v1.53 software, Inc.). Relative band intensities were normalized to β-actin.

Statistical analysis. Experiments were performed with multiple independent replicates as indicated in the figure legends (typically, n=8 for *in vivo* studies and n=3 for *in vitro* assays). Data are expressed as mean ± SEM. Statistical analyses were performed using SPSS v11.0 (SPSS, Inc.). One-way ANOVA followed by Tukey's post-hoc test was applied. $P<0.05$ was considered to indicate a statistically significant difference.

Results

Naringin ameliorates clinical symptoms of UC in DSS-induced mice. To evaluate whether oral administration of naringin could ameliorate intestinal damage in UC mice, the present study established a DSS-induced colitis model and assessed clinical and pathological indicators, including body weight, diarrhea, bloody-stool incidence colon length and macroscopic injury. Compared with the normal group, DSS-treated mice in the control group exhibited a notable reduction in body weight (Fig. 1A) and a marked increase in DAI (Fig. 1B). In addition, DSS administration caused significant colon shortening ($P<0.01$; Fig. 1C and D) and a significant increase in macroscopic injury score ($P<0.01$; Fig. 1E). Notably, naringin treatment effectively alleviated these pathological changes ($P<0.01$), indicating its protective effect against DSS-induced UC. The positive control drug, mesalazine, showed a comparable protective efficacy in ameliorating these clinical symptoms (Fig. 1A-E).

Naringin suppresses histological injury in DSS-induced colitis in mice. The present study subsequently evaluated the effects of naringin on colorectal histopathology in mice with DSS-induced UC (Fig. 2A). Compared with in the normal group, DSS-treated mice exhibited severe mucosal damage, including epithelial disruption, erosion, crypt abscesses and extensive inflammatory cell infiltration (primarily neutrophils and lymphocytes). Both naringin and mesalazine treatments markedly ameliorated these pathological features, preserving mucosal and crypt architecture.

Pathological scoring further supported these observations ($P<0.01$; Fig. 2B). Compared with the normal group, DSS treatment significantly increased histological scores. Treatment with either naringin or mesalazine significantly reduced these scores compared with the DSS group.

Naringin repairs intestinal mucosa and decreases JAK2/STAT3 signaling pathway-related protein expression in DSS-induced colitis in mice. The JAK2/STAT3 signaling pathway is abnormally activated in patients with UC and is known to exacerbate colonic inflammation and compromise mucosal barrier function (26,27). Consistent with this, western blot analysis revealed a significant upregulation of p-JAK2 and p-STAT3, as well as significantly elevated IL-6 expression, in DSS-induced mice compared with the normal group. Notably, treatment with naringin or mesalazine significantly suppressed the activation of JAK2/STAT3, as evidenced by reduced p-JAK2 and p-STAT3 levels, and significantly reduced IL-6 expression, showing a clear difference compared with the model group ($P<0.05$; Fig. 3B-H).

Tight junction proteins are important structural components of the intestinal mucosal barrier and are closely linked to the pathogenesis of UC. Among these, ZO-1 and occludin serve important roles in maintaining epithelial integrity (28,29). To further investigate the protective effects of naringin, the present

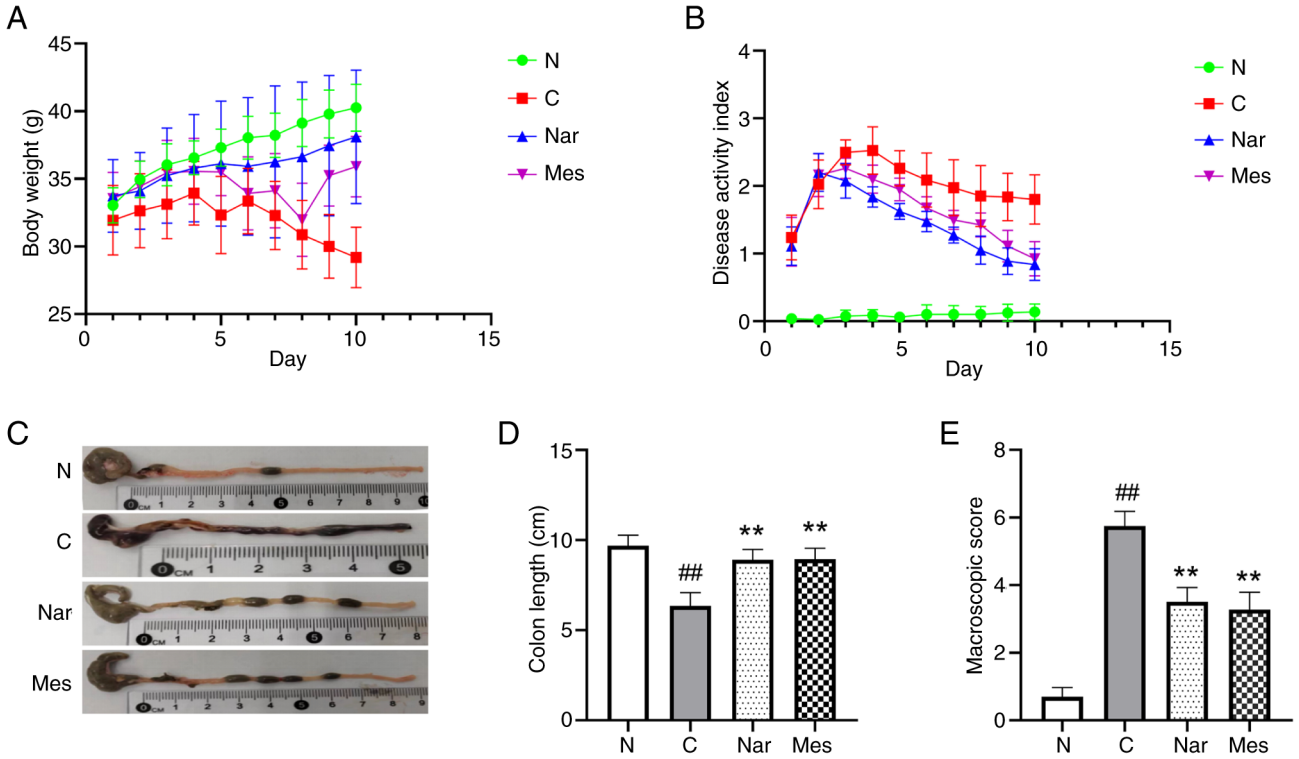

Figure 1. Naringin ameliorates clinical symptoms in DSS-induced ulcerative colitis mice. (A) Body weight changes during 10-day DSS exposure. (B) Disease activity index changes during 10-day DSS exposure. (C) Representative colon images; scale bar, 1 cm. (D) Colon length quantification. (E) Macroscopic injury scores. Data are presented as mean ± SEM. n=8. **P<0.01 vs. control group; $^{\#\#}$P<0.01 vs. normal group. One-way ANOVA followed by Tukey's post-hoc test was applied. N, normal group; C, control group; Nar, naringin group; Mes, mesalazine group; DSS, dextran sulfate sodium.

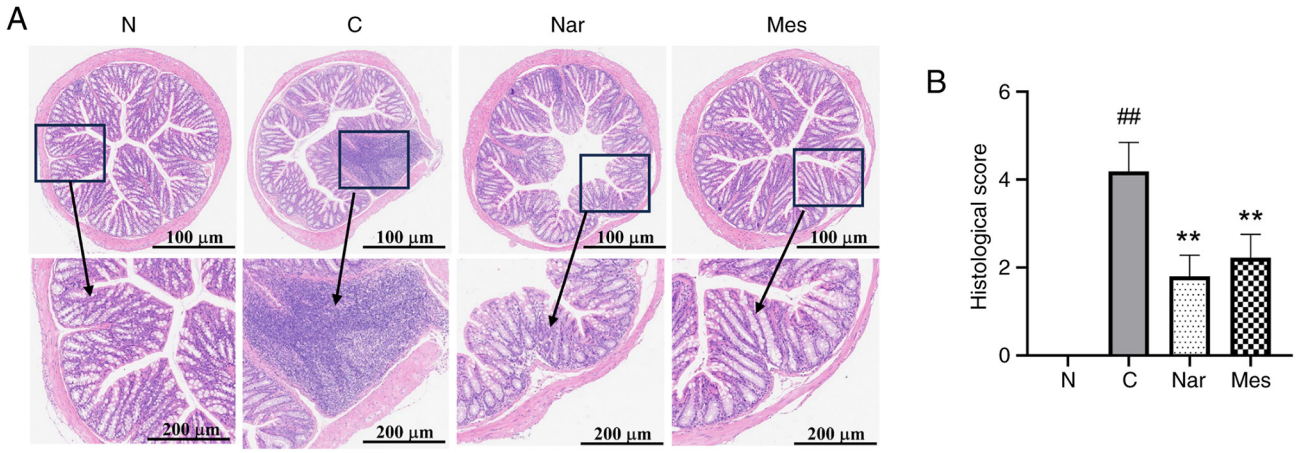

Figure 2. Naringin attenuates histological damage in dextran sulfate sodium-induced colitis mice. (A) Representative hematoxylin and eosin-stained colon sections from each group. Scale bar, 100 (overview) and 200 μm (zoomed-in view). (B) Histopathological scores of colon sections from each group. n=8. Data are presented as mean ± SEM. **P<0.01 vs. control group; $^{\#\#}$P<0.01 vs. normal group. One-way ANOVA followed by Tukey's post-hoc test was applied. N, normal group; C, control group; Nar, naringin group; Mes, mesalazine group.

study assessed their expression in colonic tissues. Naringin treatment significantly increased the expression of both ZO-1 and occludin in UC mice, with levels significantly higher than those in the DSS model group (P<0.01; Fig. 3I and J). Similarly, mesalazine treatment significantly upregulated the expression of these tight junction proteins compared with the DSS group. As expected, the expression levels of ZO-1 and occludin in the DSS control group were significantly lower than those in the normal group.

Naringin repairs IL-6-induced barrier injury in Caco-2 cells. The intestinal mucosal barrier is an important component of host defense, and its disruption in patients with UC leads to impaired barrier function and pathological immune activation. A decrease in TEER is widely recognized as an indicator of barrier dysfunction (30,31). To evaluate the protective effect of naringin, the present study established an IL-6-induced barrier injury model in Caco-2 monolayers. After 10 days of culture, confluent Caco-2 cells formed a resistant monolayer with a baseline TEER of 927.9

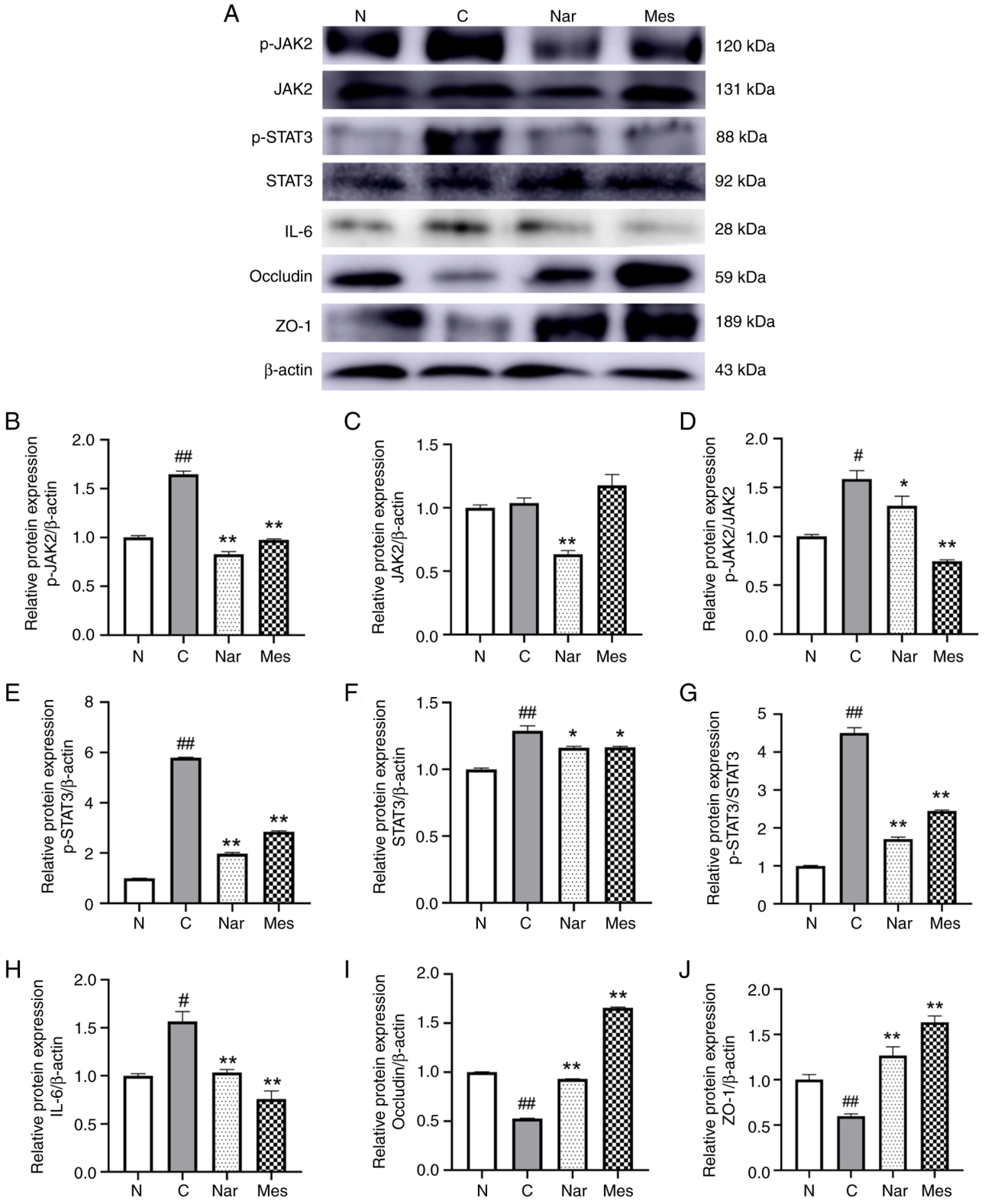

Figure 3. Naringin inhibits JAK2/STAT3 signaling and restores tight junction proteins in dextran sulfate sodium-induced colitis. (A) Representative western blotting images of p-JAK2, JAK2, p-STAT3, STAT3, IL-6, occludin, ZO-1 and β-actin expression in colon tissues. Densitometric semi-quantification of the relative protein expression levels of (B) p-JAK2/β-actin, (C) JAK2/β-actin, (D) p-JAK2/JAK2, (E) p-STAT3/β-actin, (F) STAT3/β-actin, (G) p-STAT3/STAT3, (H) IL-6/β-actin, (I) occludin/β-actin and (J) ZO-1/β-actin. Data are presented as mean ± SEM. n=3. *P<0.05 and **P<0.01 vs. control group; $^{\#}$P<0.05 and $^{\#\#}$P<0.01 vs. normal group. One-way ANOVA followed by Tukey's post-hoc test was applied. N, normal group; C, control group; Nar, naringin group; Mes, mesalazine group; p-, phosphorylated; JAK2, Janus kinase 2; STAT3, signal transducer and activator of transcription 3; IL-6, ZO-1, zona occludens-1.

Ω/cm^2. IL-6 stimulation caused a significant decrease in TEER, providing evidence of impaired barrier integrity. Treatment of IL-6 stimulated cells with naringin significantly restored TEER values compared with the IL-6 group, whereas naringin alone did not alter TEER in unstimulated cells compared with the normal group (P<0.01; Fig. 4A).

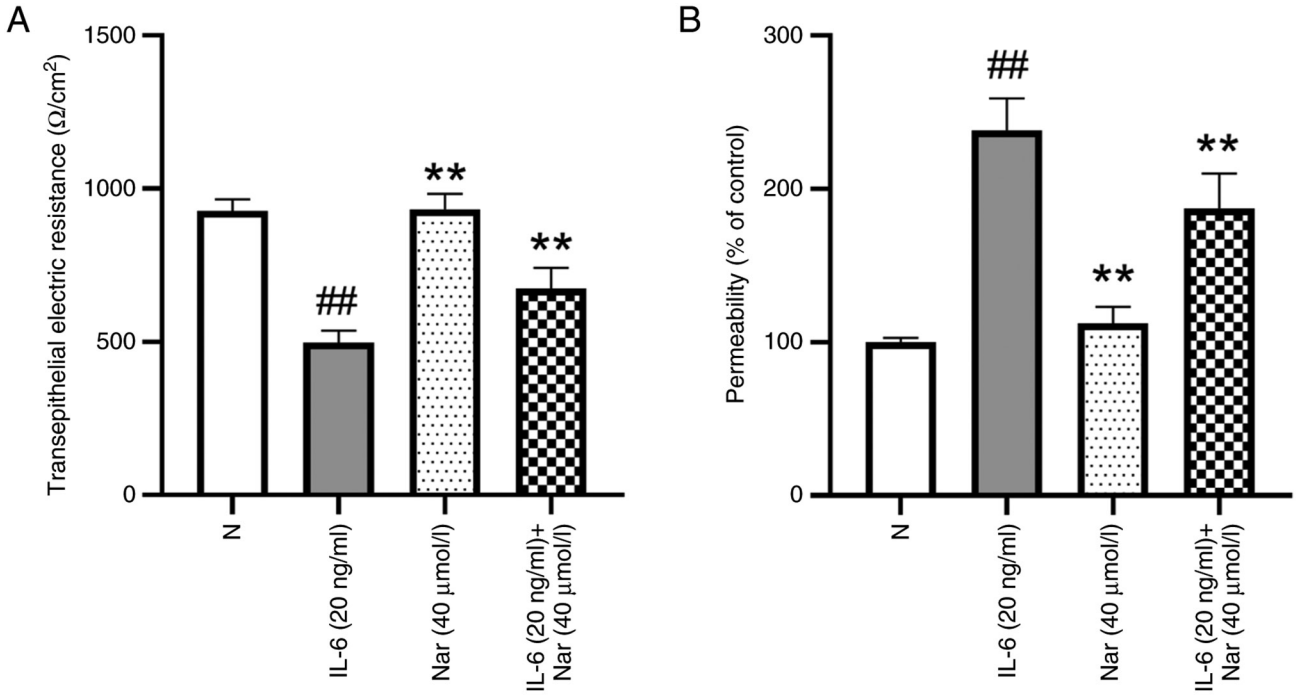

Figure 4. Naringin restores barrier function in IL-6-induced Caco-2 cells. (A) Transepithelial electrical resistance values over time. (B) Fluorescein isothiocyanate-dextran 4 kDa permeability assay. n=6. Data are presented as mean ± SEM. **P<0.01 vs. IL-6 group; $^{\#\#}$P<0.01 vs. normal group. One-way ANOVA followed by Tukey's post-hoc test was applied. Nar, naringin.

To further assess barrier permeability, FD-4 was added to the upper chamber of Transwell inserts. In IL-6-treated cells, FD-4 transport into the lower chamber increased 2.3-fold compared with the normal group, indicating elevated paracellular permeability. Naringin co-treatment significantly reduced FD-4 flux compared with the IL-6 group (P<0.01; Fig. 4B). Together, these results demonstrate that naringin effectively repairs IL-6-induced barrier damage in Caco-2 cells.

Naringin enhances fluorescent expression of tight junction proteins in Caco-2 cells. A previous study has shown that naringin can enhance the mRNA expression of tight junction proteins ZO-1 and occludin in Caco-2/RAW264.7 co-culture systems (18). To further clarify whether the mucosal protective effect of naringin was related to the JAK2/STAT3 signaling pathway, the present study used IL-6 to induce mucosal damage in cells and used STAT3 gene silencing to examine the mechanism of action of naringin. Tight junction protein expression was assessed using immunofluorescence (Fig. 5), and JAK2/STAT3 pathway activation was evaluated using western blot analysis (Fig. 6).

Immunofluorescence analysis revealed that in the normal group, ZO-1 (blue) and occludin (green) displayed strong, continuous fluorescence signals along cell-cell junctions, reflecting intact tight junctions. IL-6 stimulation significantly reduced the fluorescence intensity of both proteins compared with the normal group (P<0.01), indicating barrier disruption. Naringin treatment significantly alleviated this reduction, restoring ZO-1 (P<0.01) and occludin (P<0.05) expression at cell borders. Notably, the combination of STAT3 silencing and naringin treatment (IL-6 + Nar + siSTAT3 group) also significantly restored the fluorescence intensities of ZO-1 and occludin compared with those in the IL-6 group (P<0.01), to a level comparable with that achieved by naringin alone (Fig. 5). This supports the conclusion that naringin-induced protection of tight junctions is mediated, at least in part, through the inhibition of JAK2/STAT3 signaling (Fig. 5).

Western blot analysis showed that IL-6 stimulation significantly increased the expression of p-JAK2 (P<0.01; Fig. 6C and E) and p-STAT3 (P<0.01; Fig. 6F and H) in Caco-2 cells compared with the normal group, while JAK2 and STAT3 levels remained largely unchanged (P>0.05; Fig. 6D and G). Transfection with siSTAT3 alone significantly reduced total STAT3 protein levels compared with siNC transfection (P<0.01; Fig. 6B), confirming knockdown efficiency. Naringin treatment significantly reduced the expression of p-JAK2 and p-STAT3 relative to the IL-6 group (P<0.05; Fig. 6C, E, F, H). The present study subsequently examined the effect of STAT3 silencing in the context of IL-6 and naringin treatment. Compared with in the IL-6 group, the combination treatment of naringin and STAT3 siRNA (IL-6 + Nar + siSTAT3) led to a significant reduction in both p-JAK2 (P<0.01; Fig. 6C and E) and p-STAT3 levels (P<0.05; Fig. 6F and H).

However, when compared specifically to the IL-6 + Nar group, the combination treatment (IL-6 + Nar + siSTAT3) significantly decreased p-STAT3 levels (P<0.05; Fig. 6H). By contrast, p-JAK2 levels were significantly increased in the IL-6 + Nar + siSTAT3 group relative to the IL-6 + Nar group (P<0.01; Fig. 6E). An increase in total STAT3 protein was observed in both siRNA co-treatment groups (IL-6 + Nar + siSTAT3 and IL-6 + Nar + siNC) compared with that in the normal, IL-6 and IL-6 + Nar groups (P>0.05; Fig. 6G), which may represent a compensatory cellular response. Despite this increase in total STAT3, JAK2/STAT3 pathway activity (i.e., the phosphorylation levels of JAK2 and STAT3,

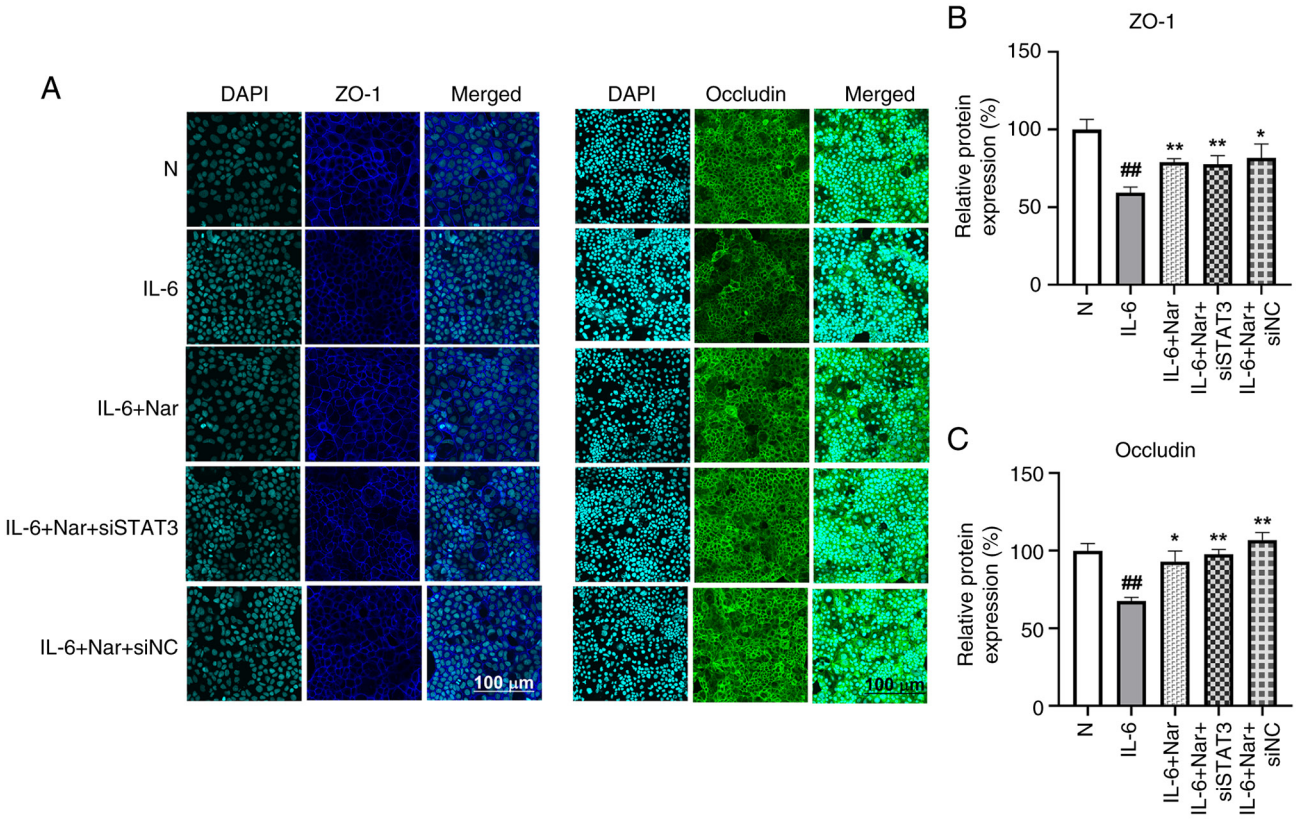

Figure 5. Naringin reverses IL-6-induced ZO-1 and occludin impairment in a STAT3-dependent manner. (A) Immunofluorescence staining for ZO-1 (blue) and occludin (green); nuclei were stained with DAPI (cyan). Merged shows the merged images of DAPI and respective protein staining. Quantitative analysis of relative (B) ZO-1 and (C) occludin protein expression. (n=3). Data are presented as mean ± SEM. *P<0.05 and **P<0.01 vs. IL-6 group; $^{\#\#}$P<0.01 vs. normal group. One-way ANOVA followed by Tukey's post-hoc test was applied. ZO-1, zona occludens-1; N, normal group; Nar, naringin; STAT3, signal transducer and activator of transcription 3; si, small interfering RNA; NC, negative control.

semi-quantified as p-JAK2/JAK2 and p-STAT3/STAT3 ratios) in the IL-6 + Nar + siSTAT3 group remained significantly suppressed compared with in the IL-6 group (P<0.01; Fig. 6E and H). Furthermore, analysis of tight junction proteins showed that naringin treatment (IL-6 + Nar) increased the expression of both occludin and ZO-1 compared with in the IL-6 group (P<0.01; Fig. 6I and J). Notably, the combination treatment with STAT3 silencing (IL-6 + Nar + siSTAT3) differentially affected the two proteins: It further enhanced occludin expression but reduced ZO-1 expression relative to the IL-6 + Nar group. This suggests a complex regulatory role of STAT3 in modulating distinct tight junction components.

Discussion

UC is a chronic, non-specific inflammatory disease of the gastrointestinal tract that primarily affects the colon and rectum, and is commonly characterized by abdominal pain, diarrhea and bloody stool (32,33). Current pharmacological interventions, such as sulfonamides, corticosteroids and immunosuppressive agents, can alleviate UC symptoms; however, high recurrence rates and limited long-term efficacy remain notable clinical challenges (34,35). Consequently, the development of effective strategies for treating and preventing UC has attracted considerable attention globally (34,36). *Citrus aurantium* L., dried immature orange, possesses both nutritional and medicinal value, with flavonoids representing its principal bioactive constituents. Naringin, the dominant flavonoid, exhibits multiple pharmacological activities (17,37). Previous studies have shown that naringin suppresses jejunal contractions, alleviates intestinal spasms (19), enhances the repair of TNBS-induced intestinal mucosal barrier damage in experimental mice, downregulates inflammatory factors such as iNOS, COX-2 and TNF-α, and preserves cellular permeability and integrity (18) in IBD models. These findings suggest that naringin may exert protective effects in UC, thereby supporting its clinical potential as a food-derived therapeutic agent.

In experimental UC models, the DAI provides a comprehensive measure of disease severity by integrating weight loss, stool consistency and presence of blood (38,39). Colon shortening is another hallmark of DSS-induced UC and serves as a reliable morphological indicator of disease severity (33,40). In the present study, DSS administration markedly increased DAI scores and significantly reduced colon length compared with the normal group. Naringin treatment ameliorated these parameters, indicating a protective effect. Histopathological analysis further revealed that naringin alleviated epithelial necrosis, goblet cell loss, crypt destruction and inflammatory infiltration in DSS-treated mice.

Mechanistically, the present study demonstrated that naringin protected against UC by inhibiting the JAK2/STAT3 signaling pathway and enhancing intestinal barrier integrity. Tight junction proteins such as ZO-1 and occludin are

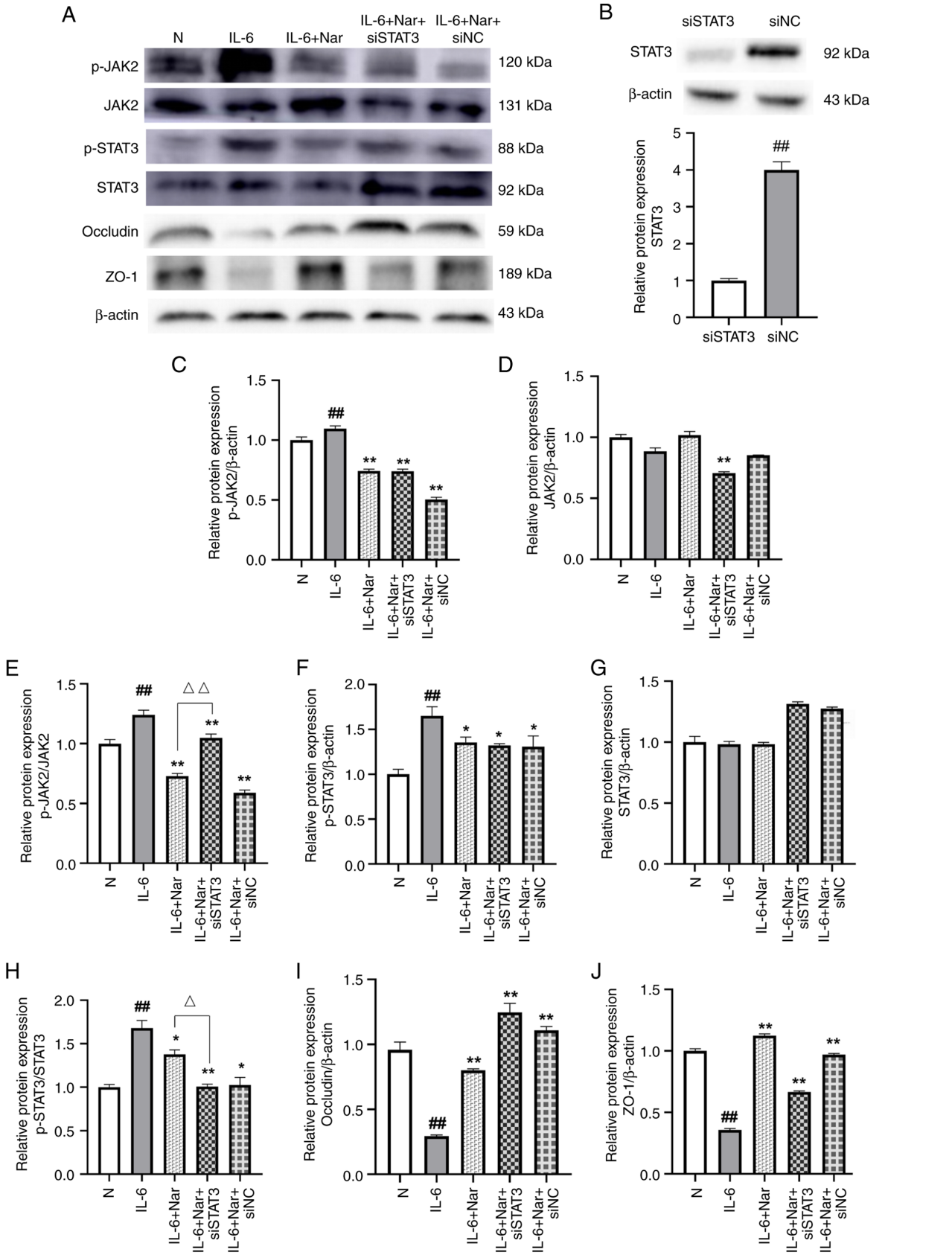

Figure 6. Naringin suppresses JAK2/STAT3 activation in IL-6-stimulated Caco-2 cells with STAT3 silencing. (A) Western blot analysis of p-JAK2, JAK2, p-STAT3, STAT3, occludin and ZO-1 in Caco-2 cells under indicated treatments. (B) Validation of STAT3 knockdown efficiency: Relative STAT3 expression in cells transfected with siSTAT3 vs. siNC. $^{\#\#}$P<0.01 vs. siNC. Densitometric semi-quantification of relative protein expression levels of (C) p-JAK2/β-actin, (D) JAK2/β-actin, (E) p-JAK2/JAK2, (F) p-STAT3/β-actin, (G) STAT3/β-actin, (H) p-STAT3/ STAT3, (I) occludin/β-actin, (J) ZO-1/β-actin. Data are presented as mean ± SEM. n=3. *P<0.05 and **P<0.01 vs. IL-6 group; $^{\#\#}$P<0.01 vs. normal group; $^{\Delta}$P<0.05 and $^{\Delta\Delta}$P<0.01 IL-6 + Nar group vs. IL-6 + Nar + siSTAT3 group. One-way ANOVA followed by Tukey's post-hoc test was applied. N, normal group; Nar, naringin group; Mes, mesalazine group; p-, phosphorylated; JAK2, Janus kinase 2; STAT3, signal transducer and activator of transcription 3; ZO-1, zona occludens-1; si, small interfering RNA; NC, negative control.

important for barrier function, and their disruption leads to increased permeability, microbial translocation and sustained inflammation (8-11). The data of the present study showed that naringin upregulated ZO-1 and occludin expression while suppressing phosphorylation of JAK2 and STAT3 in colon tissue and IL-6-stimulated Caco-2 cells. These findings suggest that naringin restores intestinal barrier integrity through JAK2/STAT3 inhibition.

The JAK2/STAT3 signaling pathway serves a dual role in UC. In inflamed intestinal tissues of patients with UC, this pathway is excessively activated and serves as a key driver of disease progression. However, in healthy intestinal epithelial cells, the activation of STAT3 can promote the repair of the intestinal mucosal barrier (15,23,41). The present study focused on UC mouse intestinal tissue and Caco-2 cells, which are fundamentally different from intestinal epithelial cells; thus, the JAK2/STAT3 signaling pathway observed in Caco-2 primarily reflected its role in promoting inflammatory reactions. This interpretation was consistent with multiple previous reports (22,42,43). ZO-1 and occludin are important proteins in the tight junction structures of the intestinal barrier, and their expression and distribution are usually used to assess the function of the intestinal barrier in the colon (12-14). The present data demonstrated that naringin upregulated ZO-1 and occludin expression while suppressing phosphorylation of JAK2 and STAT3, highlighting its potential as a dietary intervention for UC. Future studies are warranted to explore the efficacy of the clinical translation of naringin.

JAK2 is an important tyrosine protein kinase that serves an important role in the inflammatory cascade of UC, while STAT3 is a key transcription factor involved in cell proliferation, differentiation, apoptosis and the immune and inflammatory response (44). Accumulating evidence indicates that activation of the JAK2/STAT3 pathway exacerbates UC symptoms (45,46). In the present study, IL-6 was selected to induce mucosal barrier damage and inflammatory responses in Caco-2 cells, as it is a primary activator of the JAK2/STAT3 pathway (15,45). Although lipopolysaccharide is commonly used to model inflammation, it primarily activates Toll-like receptor 4/NF-κB signaling; therefore, IL-6 was more appropriate for studying JAK2/STAT3-specific effects. Furthermore, IL-6 is elevated in patients with UC and contributes to barrier dysfunction. By silencing the STAT3 gene the protective effect of naringin on this pathway was explored. IL-6 binds to its soluble receptor, forms a complex with membrane-bound glycoprotein 130, activates JAK2, induces STAT3 phosphorylation and activates downstream transcription factors, regulating the expression of inflammatory cytokines and thus mediating the occurrence of inflammatory responses (15).

The results of the present study showed that naringin significantly reduced the levels of p-JAK2 and p-STAT3 in the colon tissue of UC mice and inhibited JAK2/STAT3 activation in IL-6-stimulated Caco-2 cells. The enhanced suppression of pathway activation in the IL-6 + Nar + siSTAT3 group compared with the IL-6 group confirmed the involvement of the JAK2/STAT3 pathway in mediating the effects of naringin. Although the combination treatment (IL-6 + Nar + siSTAT3) reduced p-STAT3 compared with that in the IL-6 + Nar group, it did not lead to a further reduction in p-JAK2 levels, indicating a complex interaction. Nevertheless, the significant reduction in both p-JAK2 and p-STAT3 in the IL-6 + Nar + siSTAT3 group compared with the IL-6 group underscores that the therapeutic action of naringin is mediated, at least in part, through the suppression of JAK2/STAT3 signaling. Notably, in the siRNA-treated groups (IL-6 + Nar + siSTAT3 and IL-6 + Nar + siNC) under IL-6 stimulation, an increase in total STAT3 protein was observed, which may represent a compensatory cellular response to STAT3 knockdown. Furthermore, despite this increase in total STAT3 protein, the combination treatment (IL-6 + Nar + siSTAT3) still achieved notable suppression of JAK2/STAT3 phosphorylation compared with the IL-6 group. This effective uncoupling of pathway activation from total STAT3 protein levels underscored that the therapeutic benefit of naringin was achieved through suppressing the activation of the JAK2/STAT3 pathway.

Laser confocal microscopy revealed that IL-6 stimulation significantly decreased ZO-1 and occludin expression in Caco-2 cells, whereas naringin treatment significantly restored their expression. This restorative effect persisted even after STAT3 silencing, reinforcing the conclusion that naringin enhances tight junction protein expression primarily through JAK2/STAT3 inhibition, thereby repairing the intestinal mucosal barrier and exerting therapeutic effects in UC.

Inflammatory responses were evaluated indirectly through histological scoring of inflammatory cell infiltration and directly through activation assessment of the JAK2/STAT3 pathway, which functions upstream of multiple pro-inflammatory cytokines. However, direct measurement of cytokine levels, such as those of TNF-α and IL-1β, would provide additional validation. The effects of naringin on other inflammatory factors require further elucidation in subsequent studies.

Although JAK2 inhibition would provide more comprehensive mechanistic insights, experimental focus was placed on STAT3 due to resource constraints. Previous investigations on *Citrus aurantium* (17,18) have demonstrated inhibitory effects on JAK2 downstream pathways, including key inflammatory factors such as TNF-α and NF-κB. Given that naringin represents a major active component of *Citrus aurantium* (47), these findings provide biological plausibility for the approach in the present study. The direct targeting of JAK2 by naringin requires further investigation in future studies. Additionally, while naringin may potentially interact with other inflammatory pathways such as the NF-κB, MAPK or NACHT, LRR and PYD domains-containing protein 3 pathways, the present experimental design specifically focused on the JAK2/STAT3 axis based on prior evidence from *Citrus aurantium* (17,18). These limitations indicate important directions for future research. Studies employing molecular docking or surface plasmon resonance could strengthen mechanistic claims and are recommended for subsequent investigations. Further studies are warranted to explore additional mechanisms and validate direct molecular targets of naringin with the ultimate goal of comprehensively elucidating its therapeutic potential for UC.

In summary, integrated *in vitro* and *in vivo* evidence indicates that naringin, a flavonoid from the edible fruit *Citrus aurantium* L., significantly ameliorates DSS-induced UC in mice. Its therapeutic effects are mediated through suppression of the JAK2/STAT3 signaling pathway, leading

to both anti-inflammatory effects and enhanced tight junction protein expression. These findings support the potential of naringin as a food-based intervention for UC and provide a molecular basis for further mechanistic investigation. Although the JAK2/STAT3 pathway serves a notable role in UC pathogenesis, the precise mechanisms underlying naringin-induced modulation of this pathway require further elucidation.

Acknowledgements

Not applicable.

Funding

The present research was supported by the Hebei Youth Fund for Science and Technology Research in Colleges and Universities (grant no. QN2022014).

Availability of data and materials

The data generated in the present study may be requested from the corresponding author.

Authors' contributions

WH was responsible for funding acquisition, experimental design, conceptualization, writing the original draft and supervision. YaW contributed to the experimental design, assisted in the interpretation of data and critically revised the manuscript for important intellectual content. MW was contributed towards writing the original draft, reviewing and editing the manuscript, formal analysis and data curation. YA contributed to writing the original draft, reviewing and editing the manuscript, formal analysis and data curation. YL contributed towards experimental design and formal analysis. YiW was responsible for validation and data curation. CW contributed towards validation and formal analysis. MW and YA confirm the authenticity of all the raw data. All authors read and approved the final version of the manuscript.

Ethics approval and consent to participate

Animal experiments were approved by the Animal Welfare Committee of Hebei North University (approval no. HBNV20240223003) and performed according to institutional guidelines.

Patient consent for publication

Not applicable.

Competing interests

The authors declare that they have no competing interests.

References

1. Gros B and Kaplan GG: Ulcerative colitis in adults: A review. JAMA 330: 951-965, 2023.
2. Segal JP, LeBlanc JF and Hart AL: Ulcerative colitis: An update. Clin Med (Lond) 21: 135-139, 2021.
3. Pabla BS and Schwartz DA: Assessing severity of disease in patients with ulcerative colitis. Gastroenterol Clin North Am 49: 671-688, 2020.
4. Wangchuk P, Yeshi K and Loukas A: Ulcerative colitis: Clinical biomarkers, therapeutic targets, and emerging treatments. Trends Pharmacol Sci 45: 892-903, 2024.
5. Lee SD: Health maintenance in ulcerative colitis. Gastroenterol Clin North Am 49: xv-xvi, 2020.
6. Cheng WW, Liu BH, Hou XT, Meng H, Wang D, Zhang CH, Yuan S and Zhang QG: Natural products on inflammatory bowel disease: Role of gut microbes. Am J Chin Med 52: 1275-1301, 2024.
7. Zobeiri M, Momtaz S, Parvizi F, Tewari D, Farzaei MH and Nabavi SM: Targeting mitogen-activated protein kinases by natural products: A novel therapeutic approach for inflammatory bowel diseases. Curr Pharm Biotechnol 21: 1342-1353, 2020.
8. Li YY, Wang XJ, Su YL, Wang Q, Huang SW, Pan ZF, Chen YP, Liang JJ, Zhang ML, Xie XQ, *et al*: Baicalein ameliorates ulcerative colitis by improving intestinal epithelial barrier via AhR/IL-22 pathway in ILC3s. Acta Pharmacol Sin 43: 1495-1507, 2022.
9. Wu X, Wei S, Chen M, Li J, Wei Y, Zhang J and Dong W: P2RY13 exacerbates intestinal inflammation by damaging the intestinal mucosal barrier via activating IL-6/STAT3 pathway. Int J Biol Sci 18: 5056-5069, 2022.
10. Wang X, Xie X, Li Y, Xie X, Huang S, Pan S, Zou Y, Pan Z, Wang Q, Chen J, *et al*: Quercetin ameliorates ulcerative colitis by activating aryl hydrocarbon receptor to improve intestinal barrier integrity. Phytother Res 38: 253-264, 2024.
11. Niu C, Hu XL, Yuan ZW, Xiao Y, Ji P, Wei YM and Hua YL: Pulsatilla decoction improves DSS-induced colitis via modulation of fecal-bacteria-related short-chain fatty acids and intestinal barrier integrity. J Ethnopharmacol 300: 115741, 2023.
12. Zong Y, Meng J, Mao T, Han Q, Zhang P and Shi L: Repairing the intestinal mucosal barrier of traditional Chinese medicine for ulcerative colitis: A review. Front Pharmacol 14: 1273407, 2023.
13. Guo H, Guo H, Xie Y, Chen Y, Lu C, Yang Z, Zhu Y, Ouyang Y, Zhang Y and Wang X: Mo_3Se_4 nanoparticle with ROS scavenging and multi-enzyme activity for the treatment of DSS-induced colitis in mice. Redox Biol 56: 102441, 2022.
14. Wang Y, Zhang J, Zhang B, Lu M, Ma J, Liu Z, Huang J, Ma J, Yang X, Wang F and Tang X: Modified Gegen Qinlian decoction ameliorated ulcerative colitis by attenuating inflammation and oxidative stress and enhancing intestinal barrier function in vivo and in vitro. J Ethnopharmacol 313: 116538, 2023.
15. Zhao Y, Luan H, Jiang H, Xu Y, Wu X, Zhang Y and Li R: Gegen Qinlian decoction relieved DSS-induced ulcerative colitis in mice by modulating Th17/Treg cell homeostasis via suppressing IL-6/JAK2/STAT3 signaling. Phytomedicine 84: 153519, 2021.
16. Wang Y, Lai W, Zheng X, Li K, Zhang Y, Pang X, Gao J and Lou Z: Linderae Radix extract attenuates ulcerative colitis by inhibiting the JAK/STAT signaling pathway. Phytomedicine 132: 155868, 2024.
17. He W, Liu M, Li Y, Yu H, Wang D, Chen Q, Chen Y, Zhang Y and Wang T: Flavonoids from *Citrus aurantium* ameliorate TNBS-induced ulcerative colitis through protecting colonic mucus layer integrity. Eur J Pharmacol 857: 172456, 2019.
18. He W, Li Y, Liu M, Yu H, Chen Q, Chen Y, Ruan J, Ding Z, Zhang Y and Wang T: *Citrus aurantium* L. and its flavonoids regulate TNBS-induced inflammatory bowel disease through anti-inflammation and suppressing isolated jejunum contraction. Int J Mol Sci 19: 3057, 2018.
19. Wu Q, Liu Y, Liang J, Dai A, Du B, Xi X, Jin L and Guo Y: Baricitinib relieves DSS-induced ulcerative colitis in mice by suppressing the NF-κB and JAK2/STAT3 signalling pathways. Inflammopharmacology 32: 849-861, 2024.
20. Puppala ER, Aochenlar SL, Shantanu PA, Ahmed S, Jannu AK, Jala A, Yalamarthi SS, Borkar RM, Tripathi DM and Naidu VGM: Perillyl alcohol attenuates chronic restraint stress aggravated dextran sulfate sodium-induced ulcerative colitis by modulating TLR4/NF-κB and JAK2/STAT3 signaling pathways. Phytomedicine 106: 154415, 2022.
21. Yang NN, Yang JW, Ye Y, Huang J, Wang L, Wang Y, Su XT, Lin Y, Yu FT, Ma SM, *et al*: Electroacupuncture ameliorates intestinal inflammation by activating α7nAChR-mediated JAK2/STAT3 signaling pathway in postoperative ileus. Theranostics 11: 4078-4089, 2021.
22. He Z, Liu J and Liu Y: Daphnetin attenuates intestinal inflammation, oxidative stress, and apoptosis in ulcerative colitis via inhibiting REG3A-dependent JAK2/STAT3 signaling pathway. Environ Toxicol 38: 2132-2142, 2023.

23. Wen J, Yang Y, Li L, Xie J, Yang J, Zhang F, Duan L, Hao J, Tong Y and He Y: Magnoflorine alleviates dextran sulfate sodium-induced ulcerative colitis via inhibiting JAK2/STAT3 signaling pathway. Phytother Res 38: 4592-4613, 2024.
24. Duan B, Hu Q, Ding F, Huang F, Wang W, Yin N, Liu Z, Zhang S, He D and Lu Q: The effect and mechanism of Huangqin-Baishao herb pair in the treatment of dextran sulfate sodium-induced ulcerative colitis. Heliyon 9: e23082, 2023.
25. Wang J, Zhang C, Guo C and Li X: Chitosan ameliorates DSS-induced ulcerative colitis mice by enhancing intestinal barrier function and improving microflora. Int J Mol Sci 20: 5751, 2019.
26. Bao X, Tang Y, Lv Y, Fu S, Yang L, Chen Y, Zhou M, Zhu B, Ding Z and Zhou F: Tetrastigma hemsleyanum polysaccharide ameliorated ulcerative colitis by remodeling intestinal mucosal barrier function via regulating the SOCS1/JAK2/STAT3 pathway. Int Immunopharmacol 137: 112404, 2024.
27. Deng B, Wang K, He H, Xu M, Li J, He P, Liu Y, Ma J, Zhang J and Dong W: Biochanin A mitigates colitis by inhibiting ferroptosis-mediated intestinal barrier dysfunction, oxidative stress, and inflammation via the JAK2/STAT3 signaling pathway. Phytomedicine 141: 156699, 2025.
28. Ouyang F, Li B, Wang Y, Xu L, Li D, Li F and Sun-Waterhouse D: Attenuation of palmitic acid-induced intestinal epithelial barrier dysfunction by 6-shogaol in Caco-2 cells: The role of MiR-216a-5p/TLR4/NF-κB axis. Metabolites 12: 1028, 2022.
29. Qu Y, Li X, Xu F, Zhao S, Wu X, Wang Y and Xie J: Kaempferol alleviates murine experimental colitis by restoring gut microbiota and inhibiting the LPS-TLR4-NF-κB axis. Front Immunol 12: 679897, 2021.
30. Wu XX, Huang XL, Chen RR, Li T, Ye HJ, Xie W, Huang ZM and Cao GZ: Paeoniflorin prevents intestinal barrier disruption and inhibits lipopolysaccharide (LPS)-induced inflammation in Caco-2 cell monolayers. Inflammation 42: 2215-2225, 2019.
31. Spalinger MR, Sayoc-Becerra A, Santos AN, Shawki A, Canale V, Krishnan M, Niechcial A, Obialo N, Scharl M, Li J, *et al*: PTPN2 regulates interactions between macrophages and intestinal epithelial cells to promote intestinal barrier function. Gastroenterology 159: 1763-1777.e14, 2020.
32. Xiong T, Zheng X, Zhang K, Wu H, Dong Y, Zhou F, Cheng B, Li L, Xu W, Su J, *et al*: Ganluyin ameliorates DSS-induced ulcerative colitis by inhibiting the enteric-origin LPS/TLR4/NF-κB pathway. J Ethnopharmacol 289: 115001, 2022.
33. Yuan SN, Wang MX, Han JL, Feng CY, Wang M, Wang M, Sun JY, Li NY, Simal-Gandara J and Liu C: Improved colonic inflammation by nervonic acid via inhibition of NF-κB signaling pathway of DSS-induced colitis mice. Phytomedicine 112: 154702, 2023.
34. Wu Y, Jha R, Li A, Liu H, Zhang Z, Zhang C, Zhai Q and Zhang J: Probiotics (Lactobacillus plantarum HNU082) supplementation relieves ulcerative colitis by affecting intestinal barrier functions, immunity-related gene expression, gut microbiota, and metabolic pathways in mice. Microbiol Spectr 10: e0165122, 2022.
35. Jeong DY, Kim S, Son MJ, Son CY, Kim JY, Kronbichler A, Lee KH and Shin JI: Induction and maintenance treatment of inflammatory bowel disease: A comprehensive review. Autoimmun Rev 18: 439-454, 2019.
36. Wang M, Fu R, Xu D, Chen Y, Yue S, Zhang S and Tang Y: Traditional Chinese Medicine: A promising strategy to regulate the imbalance of bacterial flora, impaired intestinal barrier and immune function attributed to ulcerative colitis through intestinal microecology. J Ethnopharmacol 318: 116879, 2024.
37. Alam F, Mohammadin K, Shafique Z, Amjad ST and Asad MHHB: Citrus flavonoids as potential therapeutic agents: A review. Phytother Res 36: 1417-1441, 2022.
38. Mirsepasi-Lauridsen HC: Therapy used to promote disease remission targeting gut dysbiosis, in UC patients with active disease. J Clin Med 11: 7472, 2022.
39. Wu Y, Ran L, Yang Y, Gao X, Peng M, Liu S, Sun L, Wan J, Wang Y, Yang K, *et al*: Deferasirox alleviates DSS-induced ulcerative colitis in mice by inhibiting ferroptosis and improving intestinal microbiota. Life Sci 314: 121312, 2023.
40. Ruan Y, Zhu X, Shen J, Chen H and Zhou G: Mechanism of Nicotiflorin in San-Ye-Qing rhizome for anti-inflammatory effect in ulcerative colitis. Phytomedicine 129: 155564, 2024.
41. Tang L, Liu Y, Tao H, Feng W, Ren C, Shu Y, Luo R and Wang X: Combination of Youhua Kuijie Prescription and sulfasalazine can alleviate experimental colitis via IL-6/JAK2/STAT3 pathway. Front Pharmacol 15: 1437503, 2024.
42. Shalaby M, Abdelaziz RR, Ghoneim HA and Suddek GM: Imatinib mitigates experimentally-induced ulcerative colitis: Possible contribution of NF-kB/JAK2/STAT3/COX2 signaling pathway. Life Sci 321: 121596, 2023.
43. Yu T, Li Z, Xu L, Yang M and Zhou X: Anti-inflammation effect of Qingchang suppository in ulcerative colitis through JAK2/STAT3 signaling pathway in vitro and in vivo. J Ethnopharmacol 266: 113442, 2021.
44. Jiang M, Zhong G, Zhu Y, Wang L, He Y, Sun Q, Wu X, You X, Gao S, Tang D and Wang D: Retardant effect of dihydroartemisinin on ulcerative colitis in a JAK2/STAT3-dependent manner. Acta Biochim Biophys Sin (Shanghai) 53: 1113-1123, 2021.
45. Wang X, Huang S, Zhang M, Su Y, Pan Z, Liang J, Xie X, Wang Q, Chen J, Zhou L and Luo X: Gegen Qinlian decoction activates AhR/IL-22 to repair intestinal barrier by modulating gut microbiota-related tryptophan metabolism in ulcerative colitis mice. J Ethnopharmacol 302: 115919, 2023.
46. Voshagh Q, Anoshiravani A, Karimpour A, Goodarzi G, Tehrani SS, Tabatabaei-Malazy O and Panahi G: Investigating the association between the tissue expression of miRNA-101, JAK2/STAT3 with TNF-α, IL-6, IL-1β, and IL-10 cytokines in the ulcerative colitis patients. Immun Inflamm Dis 12: e1224, 2024.
47. Miles EA and Calder PC: Effects of citrus fruit juices and their bioactive components on inflammation and immunity: A narrative review. Front Immunol 12: 712608, 2021.